The Capability of CI-Orbitrap for Gas-Phase Analysis in Atmospheric Chemistry: A Comparison with the Cl-APi-TOF Technique

M. Riva, M. Bruggemann, D. Li, S. Perrier, C. George, H. Herrmann, T. Berndt

The capability of CI-Orbitrap for gas-phase analysis in atmospheric chemistry: A comparison with the CI-APi-TOF technique

M. Riva[†,*], M. Brüggemann[‡], D. Li[†], S. Perrier[†], C. George[†], H. Herrmann[‡], T. Berndt[‡,*]

[†] Univ Lyon, Université Claude Bernard Lyon 1, CNRS, IRCELYON, F-69626, Villeurbanne, France.

[‡] Leibniz Institute for Tropospheric Research (TROPOS), Atmospheric Chemistry Department (ACD), Permoserstr. 15, 04318 Leipzig (Germany)

Abstract

Chemical ionization Orbitrap mass spectrometry (CI-Orbitrap) represents a promising new technique for gas-phase analysis in analytical and atmospheric chemistries mainly due to its very high mass resolving power. In this work, we performed the first side-by-side comparison between a CI-Orbitrap and the widely used atmospheric pressure interface time-of-flight mass spectrometry (CI-APi-TOF) using two different chemical ionization methods, i.e., acetate-ion-based (CH_3COO^-) and aminium-ion-based ($n\text{-}C_3H_7NH_3^+$) schemes. The capability of the CI-Orbitrap at accurately measuring low concentrations of gaseous species formed from the oxidation of α-pinene was explored. Although this study reveals a lack of linearity of the CI-Orbitrap when measuring product ions at very low concentrations (< 1 x 10^6 molecules cm^{-3}), very good agreement between both techniques can be achieved by applying a newly developed linearity correction. It is experimentally shown that the correction function is independent of the reagent ion used. Thus, accurate quantification of organic compounds at concentrations as low as 1 x 10^5 molecules cm^{-3} by the CI-Orbitrap can be achieved. Finally, by means of tandem mass spectrometry, the unique capability of the Orbitrap allows the direct determination of the binding energy of cluster ions between analyte and reagent ions, that is needed for the assessment of a chosen ionization scheme.

Introduction

Biogenic and anthropogenic activities constantly release a wide variety of volatile organic compounds (VOCs) into the atmosphere.[1,2] Once emitted, VOC are rapidly oxidized to form oxidized VOCs (OVOCs) spanning a broad range of chemical formulas, and, thus, volatilities.[1,3,4] As a result, organic compounds play a key role in the formation of atmospheric aerosol by either condensing onto pre-existing aerosol particles or by forming new particles.[1,2,5,6] VOC emissions strongly impact atmospheric chemistry, human health, and Earth's climate. More specifically, a critical starting point in new particle formation (NPF) and growth is the generation of highly oxygenated multifunctional organic molecules (HOMs) through a process usually referred to as autoxidation.[7–9] In the course of the autoxidation process, peroxy (RO_2) radicals, formed via the oxidation of a VOC, undergo an intramolecular hydrogen shift reaction, ROO → QOOH, followed by the addition of molecular oxygen resulting in the formation of a new R'O_2 radical: QOOH + O_2 → OOQOOH (R´O_2) ("Q" stands for the organic group "R" after interamolecular H shift). This chain reaction can be repeated, yielding a broad diversity of products depending on the RO_2 radical termination steps.[8,10–12] As a result, HOMs can be formed efficiently at high enough yields to consider them as a significant source of condensing, or, in certain cases, even nucleating, organic components.[6–8,13–15] Finally, RO_2 chemistry not only controls the formation of HOMs and NPF but also impacts the production of secondary pollutants including O_3 and NO_2.[16] While in the last decade major breakthroughs have been achieved within the field of atmospheric oxidation processes and new particle formation,[6–8,17] a complete understanding of how VOC oxidation products contribute to new particle and SOA formation remains poorly constrained. Indeed, gas-phase oxidation processes of biogenic and anthropogenic VOCs yield a number of oxidized products resulting in extremely complex mixture of oxygenated VOCs (OVOCs). These span a wide range of chemical formulas, structures, and physicochemical properties and pose a critical challenge in detecting, quantifying, and characterizing key atmospheric species including RO_2 radicals and HOMs.

Mass spectrometric techniques have recently made enormous improvements in detecting and quantifying gaseous oxygenated species.[18–20] In particular, chemical ionization mass spectrometry (CIMS) has emerged as a prevailing tool due to its very low detection limits, good sensitivity, and

capability of measuring a wide variety of gaseous organic and inorganic species.[8,10,10,21] Chemical ionization (CI) is a soft ionization technique where the analyte is ionized via a clustering process with the reagent ion with minimal fragmentation or via proton transfer processes.[21–24] As part of the rapid development, multiple reagent ion schemes have been tested over the last few years. Due to the improvements in sensitivity and/or selectivity, a wide variety of oxygenated species, including RO_2 radicals and stabilized Criegee intermediates, can now be directly analyzed.[10,11,19,20,25,26] However, most of the CI mass spectrometers offer a rather limited mass resolving power (i.e., from 2 000 to 14 000), hindering yet a complete and unambiguous identification of the compounds of interest. Consequently, the presence of multiple overlapping ions leads to significant uncertainties that can only be partly resolved by computational techniques. To overcome these limitations, we have recently coupled a high-resolution mass spectrometer (Orbitrap) with a CI source.[30] The CI-Orbitrap combines the benefits of soft atmospheric pressure ionization with a unique mass resolving power ($R \geq 140\,000$ at *m/z* 200). In our first study we demonstrated the applicability of this new analytical method and evaluated its ability in detecting and characterizing OVOCs formed during the oxidation of two monoterpenes using nitrate-based (NO_3^-) CI.[30] Nonetheless, a direct comparison with the widely used atmospheric pressure interface time-of-flight mass spectrometry (CI-APi-TOF) has not been performed hitherto. Hence, the sensitivity as well as the linearity of the CI-Orbitrap with different reagent ions operated in the positive or negative mode need to be determined and compared to those of the CI-APi-TOF.

Within the present study, we performed the first side-by-side comparison between a CI-Orbitrap and a CI-APi-TOF applying two different chemical ionization schemes i.e., the acetate-ion-based (CH_3COO^-)[10,11] and the aminium-ion-based ($n\text{-}C_3H_7NH_3^+$)[11] product ionization. Unlike our initial study, we performed our experiments in a free-jet system designed to probe the early stage of a given reaction. A very short residence time was used as well as very low reactant conversion. As a result, RO_2 radicals are the main products and experiments are performed within atmospheric reaction conditions, where bimolecular steps are only important for relatively high RO_2/ HO_2 levels or in the presence of high enough concentrations of additives (e.g., NO). Hence, very low concentrations of RO_2 radicals and OVOCs are produced from the ozone and OH radical initiated oxidation of α-pinene

in order to ascertain the benefit and the limitation of the CI-Orbitrap. We also explored the potential of the CI-Orbitrap in evaluating the binding energies of RO_2 radicals and OVOCs clustered with acetate and aminium ($n\text{-}C_3H_7NH_3^+$) by means of tandem mass spectral analyses (MS^2).

EXPERIMENTAL SECTION

Ozonolysis and OH radical initiated oxidation of α-pinene ($C_{10}H_{16}$) were performed under dry conditions (RH < 0.1%) in air using a free-jet flow system at a temperature of 297 ± 1 K and atmospheric pressure.[10,11] This flow system allows the investigation of VOC oxidation under atmospheric conditions with negligible wall effects and a reaction time of 7.9 s. Ozone produced from a low-pressure mercury lamp or isopropyl nitrite (IPN) was premixed with air (5 L/min (STP)) and injected through the inner tube into the main gas stream (95 L/min (STP)) containing α-pinene diluted in air. Ozonolysis experiments (dark reaction) were performed in the absence of an OH scavenger, i.e., the in-situ OH radical formation from ozonolysis led to a combined O_3/OH + α-pinene reaction. In the pure OH experiments based on IPN photolysis, 8 NARVA 36W Blacklight Blue lamps were used for illuminating the flow system. All gas flows were set by means of calibrated gas flow controllers (MKS 1259/1179). The concentration of α-pinene was maintained at 5.0×10^{11} molecules cm^{-3}, while ozone and IPN were ramping up from 2.5×10^{10} to 5.6×10^{11} and from 1.7×10^{10} to 6.7×10^{11} molecules cm^{-3}, respectively.

The chemical composition of the oxygenated products was retrieved in real time by a Q-Exactive Orbitrap Plus mass spectrometer (Thermo Scientific) and a chemical ionization - atmospheric pressure interface - time-of-flight mass spectrometer (CI-APi-TOF, Tofwerk AG). Both instruments have been described elsewhere and were equipped with a similar Eisele-type inlet.[21,30–33] While the CI inlet mounted on the APi-TOF is manufactured by Airmodus (Finland), the CI inlet installed on the Orbitrap is a home-built version with minor modifications regarding to the commercially available inlet (i.e., dimensions of the drift tube and specific flange, see for more details ref.[30]). The sample flow rate for both instruments was set at ~ 10 L/min (STP). Protonated n-propylamine ($n\text{-}C_3H_7NH_3^+$) or acetate (CH_3COO^-) ions were produced using an X-ray source or an Am-241 source for the Orbitrap and the APi-TOF, respectively. In the ion-molecule-reaction (IMR) zone, the reagent ions from a clean sheath nitrogen flow were guided into the concentric sample flow by an electrical field without

turbulent mixing of both streams. The residence time within the IMR zone was in the range of 200 – 300 ms in both instruments.

The reagent ions were $(CH_3COOH)_n$-CH_3COO^- (n = 0,1) and $(n\text{-}C_3H_7NH_2)_m$-$n\text{-}C_3H_7NH_3^+$ (m = 0,1) in the negative and positive mode, respectively. RO_2 radicals as well as closed-shell products, called "prod" for all together, were detected as clusters with the respective reagent ions according to the following reactions (1) and (2):

$$(CH_3COOH)_n\text{-}CH_3COO^- + \text{prod} \rightarrow (\text{prod})\text{-}CH_3COO^- + (CH_3COOH)_n \quad (n = 0,1) \qquad (1)$$

$$(n\text{-}C_3H_7NH_2)_m\text{-}n\text{-}C_3H_7NH_3^+ + \text{prod} \rightarrow (\text{prod})\text{-}n\text{-}C_3H_7NH_3^+ + (n\text{-}C_3H_7NH_2)_m \quad (m = 0,1) \qquad (2)$$

It is important to mention that the absolute calibration of the detected oxygenated products is impossible due to a lack of authentic reference substances for RO_2 radicals and the majority of closed-shell products. Thus, the product signals of both mass spectrometers were normalized to the sum of the reagent ions, i.e., $\Sigma[(CH_3COOH)_n\text{-}CH_3COO^-$ (n = 0,1)] or $\Sigma[(n\text{-}C_3H_7NH_2)_m\text{-}n\text{-}C_3H_7NH_3^+$ (m = 0,1)]. The resulting normalized signals were used for the comparison in order to evaluate the performance of both techniques.

However, the lower end value of the calibration factor f can be calculated considering the ion-molecule reaction within the CI-inlet, $f = 1 / (k \times t \times f_{inlet})$,[34] where k is the rate coefficient of the ion-molecule reaction, t the reaction time and f_{inlet} corresponds to the "prod" loss in the sampling tube. Diffusion loss of the RO_2 radicals and OVOCs in the sampling lines to the CI-APi-TOF and the CI-Orbitrap were calculated to be 12% and 38%, respectively, assuming diffusion-controlled wall losses.[10] Taking into account this diffusion loss, $f_{inlet} = 0.88$, and a reaction time of the ion-molecule reaction t = 0.2 – 0.3 s (which is similar for both instruments), a calibration of $f_{calc} = (1.3 - 2.8) \times 10^9$ molecules cm^{-3} can be calculated. It should be mentioned that using the only reliable absolute calibration technique (i.e., sulfuric acid) a calibration factor of $f_{H2SO4,exp} = 1.85 \times 10^9$ molecules cm^{-3} was determined in previous experiments. This value is in good agreement with the range of f_{calc}. The calibration factor f of reactions (1) and (2) was set equal to $f_{H2SO4,exp}$ by practical reasons. The

uncertainty of the lower end "prod" concentrations determined according to equation (1) or (2) is assumed to be not higher than a factor of two due to the expected uncertainty of the used calibration factor $f_{H2SO4,exp} = 1.85 \times 10^9$ molecules cm^{-3}, and possible inaccuracy connected with the duty cycle correction. Therefore, only lower limit product concentrations are available based on this calculated calibration factor.

Duty cycle correction was applied for the APi-TOF data in order to account for the *m/z* discrimination during the ion extraction.[10,24,35] In the case of the CI-Orbitrap, for each experiment, the ion transmission was evaluated by comparing the loss of the number of charges of the reagent ions with the increase of the number of charges of all the ions within the *m/z* 200 – 600 Th. This simple method provides a rough estimate of the ion transmission for the compounds of interest relative to the reagent ions. As a result, a factor of 2 was applied to correct for the lower ion transmission of the reagent ions in order to determine the normalized signals.

In addition, we further evaluated the ion transmission of the Q Exactive Orbitrap in the *m/z* 53 – 800 Th using the depletion method described by Heinritzi et al.[36] This method takes into consideration losses within the inlet as well as the different ion optics and C-Trap (see Figure S1). In short, 4 different perfluorinated acids were introduced into the mass analyzer in order to deplete the reagent ions. As a result, the relative transmission efficiency can be obtained by comparing the decrease of signal strength of the reagent ions with the rising signals from the perfluorinated acids at larger masses (see supplementary information for more details). The relative ion transmission was only determined for the Q-Exactive Orbitrap using nitrate-ion based chemistry. It should be pointed out that the depletion method leads to significantly different results for the ion transmission of a mass spectrometer than absolute calibration methods.[7,36–38] Nevertheless, the results of the depletion method provide a first insight into the ion transmission of a Q Exactive Orbitrap.

The Q Exactive Plus Orbitrap (Orbitrap-Tropos) was used in positive (i.e., $n\text{-}C_3H_7NH_3^+$) and negative mode (i.e., CH_3COO^-) and connected to the free-jet flow system. The Q Exactive Orbitrap (Orbitrap-IRCELYON) was solely used in negative mode (NO_3^-) to determine the ion transmission and to developed the linearity correction. Both instruments were operated using the same settings and were run in full scan mode with a high mass resolving power of 140 000 (at *m/z* 200 Th), allowing an

identification of a wide variety of species. The instruments were operated in negative or positive mode, scanning from *m/z* 50 to 750 Th with an automatic gain control (AGC) target of 1 x 10^5 charges, a maximum injection time of 1 s, resulting in a scan rate of 0.2 scans/s. Spectra were averaged of 5 microscans (1 microscan corresponding to 1 ion injection). The stacked-ring ion guide (or S-Lens) is a radio frequency (RF) device efficiently capturing and focusing the ions into a tight beam. As previously described it contains a series of electrodes where voltages are applied in order to focus the ions. The S-lens level was maintained at 60%, to maximize ion transmission and the limit of detection. The C-Trap consist of a RF-based ion collecting trap (Figure S1), which is automatically controlled by the AGC (automatic gain control) in order to prevent space-charge effects. In order to evaluate the impact of the number of charges collected in the C-trap, the AGC target of the Orbitrap-Tropos instrument was scanned from 5 x 10^4 to 1 x 10^6 charges. External mass calibrations were performed prior to the experiments by injecting a 2 mM sodium acetate solution using an electrospray ionization source. This procedure provided a suite of negative and positive adduct ions in the desired mass range of *m/z* 59 – 700 Th. Tandem mass spectral (MS^2) analyses were performed by ramping up the normalized collision energy (NCE) from 1 – 7 eV (i.e., normalized to singly charged ions at *m/z* 500). Thus, to retrieve the collision energy (CE) encountered by ions at any given *m/z* ratio within the higher-energy collision dissociation (HCD) cell, the CE can be calculated as follows: CE = (*m/z* / 500) x NCE x f, where f stands for the number of charges of the ion. To ensure an optimal detection of the product ions, the mass spectra obtained using the CI-APi-TOF and the CI-Orbitrap were averaged over 10 minutes each. A time resolution of 5 min was used for the MS^2 analyses conducted by the Orbitrap. The high-resolution Orbitrap data were analyzed by XCalibur 4.1 (Thermo Scientific) software package to determine accurate composition and the abundance of the compounds of interest. Peak fitting of the CI-APi-TOF data was performed by means of the Matlab-based toftools software.[37]

RESULTS AND DISCUSSION

Characterization of the CI-Orbitrap. Despite the wealth of studies using the Orbitrap technique, little is known about the capability of the Orbitrap in measuring compounds on-line at low concentrations. For example it has been reported that the Orbitrap can provide a non-linear response,

potentially impacting isotope ratios, determination and the quantification of compounds present at extremely low concentrations.[39] In view of these findings available from literature, we evaluated the performance of the CI-Orbitrap by comparing the measured vs. the theoretical isotopic intensities using product ions analyzed by the Orbitrap-Tropos using protonated n-propylamine (n-$C_3H_7NH_3^+$) and acetate (CH_3COO^-). To further estimate the impact of different reagent ions, results from our former study performed with the Orbitrap-IRCELYON using nitrate-ion based chemistry[30] are also compared here. In both cases, OVOCs were continuously generated in the flow tube from either the ozonolysis and/or OH radical initiated oxidation of α-pinene. Hence, the abundance of the main OVOCs (e.g., $C_{10}H_{14,16}O_x$; $C_{20}H_{30,32}O_x$) and RO_2 radicals (e.g., $C_{10}H_{15,17}O_x$) at nominal masses M, (M + 1) and (M + 2), corresponding to their ^{13}C atom and ^{18}O atom fraction, were measured to cover a wide range of normalized product signals in the range of 5×10^{-7} to 5×10^{-2}. Signal intensities reported in Figure 1A were obtained with an AGC target of 1×10^5 charges. As depicted in Figure 1A, when the ratio is equal to 1.0 for normalized signal > ~ 4×10^{-4} to (~ 1×10^6 molecules cm^{-3}), the Orbitrap is providing a linear measure of the ion intensity. However, this ratio dropped significantly for normalized signals below ~ 4×10^{-4}. Such a situation occurs when the ion intensity is close to the instrumental threshold, i.e., by using standard settings the Orbitrap mass analyzer records only signals if S/N > 1.3. The ion signals below this threshold are treated as undetected by the acquisition software. Due to the statistics, peaks with an average S/N = 1.5 for example will appear above this threshold only in a limited amount of cases reducing the resulting peak intensity.[40] As a result, for a normalized signal smaller than 1×10^{-5}, the CI-Orbitrap only detects 5 – 10 % of the "true ion number distribution". That means, using the instrumental parameters and the calibration factor employed here (1.85×10^9 molecules cm^{-3}) the limit of quantification (LoQ, corresponding to lowest normalized signal observed within the linear range) of the Orbitrap was evaluated to be ~ 1×10^6 molecules cm^{-3} at a 10-minute integration time. It is worth pointing out that the limit of detection (LoD, corresponding to the lowest normalized signal observed) is likely one or two orders of magnitude lower than the LoQ but due to the lack of linearity accurate numbers cannot be directly provided. By adjusting the AGC target the linear range can be shifted towards lower ion concentrations as shown in Figure 1B. This can be explained by larger number of ions trapped within the C-trap prior to the Orbitrap scan

resulting in more ions entering the Orbitrap mass analyzer. This leads to an enhanced S/N ratio and better statistics. Hence, we have evaluated the impact of the AGC target (scanned from 5 x 10^4 to 1 x 10^6 charges) on the linearity and found that by optimizing the AGC target, the LoQ of the CI-Orbitrap is anticipated to be greatly extended. However, as most of our previous experiments were performed using an AGC target of 1 x 10^5 charges, we kept this setting to perform the side-by-side comparison.

Comparison CI-Orbitrap vs CI-APi-TOF. To evaluate the performance of the CI-Orbitrap compared to the widely used CI-APi-TOF technique we directly performed side-by-side experiments. Both instruments, equipped with a similar type of inlet originally designed by Eisele et al.[31] and running with the same reagent ion, sampled concurrently RO_2 radicals as well as OVOCs produced under well-controlled reaction conditions. We focused on the detection of RO_2 radicals produced from the oxidation of α-pinene. Using acetate and aminium ($n\text{-}C_3H_7NH_3^+$) as the reagent ions, the main RO_2 radicals from α-pinene oxidation, $HO\text{-}C_{10}H_{16}(O_2)_\alpha O_2$ (α = 0, 1, 2), were detected by means of the CI-Orbitrap, in line with the findings of the CI-APi-TOF.[24,30,35] As depicted in Figures 2 and S2, the mass resolving power of the Orbitrap can accurately distinguish the different species, which is often impossible with typical TOF mass analyzers. To further illustrate the difference, we have directly compared ion signals measured by the CI-Orbitrap and by the CI-APi-TOF equipped with a high resolution mass analyzer (HR-TOF, resolution ~ 3000) (Figure 2).

Figure 3 shows the results of the OH radical-initiated oxidation of α-pinene. The OH radicals were generated by isopropyl nitrite (IPN) photolysis. The formation of the additional RO_2 radical $HO\text{-}C_{10}H_{15}(OH)(O_2)O_2$ can be explained by the reaction of $HO\text{-}C_{10}H_{16}(O_2)_2O_2$ with NO and subsequent radical isomerization as discussed in a former study.[35] NO is formed from the IPN photolysis. In addition to the RO_2 radicals, also closed-shell products were detected including carbonyls and organic nitrates produced from the RO_2 + NO reactions.[16] Lastly, products arising from other bimolecular RO_2 reactions were not detected or were below the detection limit under the selected experimental conditions due to the relatively low RO_2 radical concentrations < 10^8 molecules cm^{-3} and the very short reaction time of 7.9 s.

As shown in Figure 3, for uncorrected normalized intensities above (2 – 3) × 10^{-4} (corresponding to ~ (4 – 6) × 10^5 molecules cm^{-3}) both techniques are in very good agreement. The lack

of linearity hampers the Orbitrap, unlike the APi-TOF, to accurately measure lower concentrations. However, this lack of linearity appears to be independent of the instrument and the type of reagent ions (Figure 1A). This behavior indicates that this instrumental limitation can be overcome in order to retrieve the "correct" signal strength for peaks with lowest signal intensity. Indeed, using all measurements from multiple experiments and reagent ions, a function named "sigmoidal correction function" based on a fitting algorithm using a characteristic sigmoidal shape can be determined. Therefore, raw normalized signals (corrected for sampling losses) measured with the CI-Orbitrap were further corrected using the "sigmoidal correction function", see also Figure 1. By applying this method, all the data were corrected (open markers), which greatly helps maintaining the good agreement between both techniques (Figure 3). However, for uncorrected signal intensities below a threshold of $5 \times 10^{-6} - 1 \times 10^{-5}$ this approach results in an overestimation of the ion concentrations as the signal is likely very close to the noise level of the instrument. As a result, such data points were not included in Figures 3, 4, S3 and S4. While the APi-TOF can further help correcting this lack of linearity we preferred to propose a method based only on the signal acquired by the Orbitrap. Hence, the reported LoD is likely an upper limit and might be even pushed further with appropriate and collocated instrumentations.

Overall, product signals measured by CI-Orbitrap and the CI-APi-TOF are mostly within a factor of 2 (Figure 5) providing a good agreement between these two analytical techniques for corrected normalized signal intensity ranging from ~ 5×10^{-5} to 1×10^{-2} (corresponding to ~ 1×10^{5} to 2×10^{7} molecules cm^{-3}). Exception are the measurements of highly oxidized products using acetate ionization. The reason for that is not clear at the moment. It is worth pointing out that the positive mode measurements were less impacted by the lack of linearity compared to negative mode measurements. This is explained by the fact that at a given product concentration, the resulting ion intensity measured by aminium ($n\text{-}C_3H_7NH_3^+$) ionization is much greater than for acetate ionization. In the case of the highest oxidized RO_2 radicals, i.e., $HO\text{-}C_{10}H_{16}(O_2)_2O_2$ and $HO\text{-}C_{10}H_{15}(OH)(O_2)O_2$ bearing -OH and -OOH moieties, the obtained corrected signal intensities are almost identical within a factor of two applying either acetate or aminium ($n\text{-}C_3H_7NH_3^+$) for product ionization. This fact is obviously due to strong binding of these RO_2 radicals to both reagent ions. Thus, a near-maximum

detection sensitivity can be expected for these reagent ions.[41,42] On the other hand, for the less oxidized RO_2 radicals HO-$C_{10}H_{16}O_2$ and HO-$C_{10}H_{16}(O_2)O_2$ the detection sensitivity based on aminium (n-$C_3H_7NH_3^+$) ionization is definitely higher compared to acetate ionization, i.e., by a factor of 500 – 1000 in the case of HO-$C_{10}H_{16}O_2$.[42]

Ozonolysis experiments in the absence of an OH scavenger were conducted in order to generate a larger variety of products, mainly RO_2 radicals, formed from the simultaneous ozone and OH radical reactions of α-pinene. Accordingly, two types of RO_2 radicals have been formed, i.e., the ozonolysis-derived RO_2 radicals O,O-$C_{10}H_{15}(O_2)_xO_2$ (x = 0, 1, 2, 3) and the OH-derived RO_2 radicals HO-$C_{10}H_{16}(O_2)_\alpha O_2$ (α = 0, 1, 2).[7,35] Figure 4 presents the signal intensities of both types of RO_2 radicals measured by means of aminium (n-$C_3H_7NH_3^+$) ionization. While the agreement for the most oxidized RO_2 radicals is again very good, the signals of the less oxidized species O,O-$C_{10}H_{15}O_2$ and HO-$C_{10}H_{16}O_2$ (Figures 3 and 4) are systematically higher using the CI-Orbitrap by a factor of two or higher. In contrast, for the most oxidized RO_2 the difference between the two instruments was only ~ 20%. Such a disparity might be explained by less efficient declustering of the relatively weakly bound aminium clusters of O,O-$C_{10}H_{15}O_2$ and HO-$C_{10}H_{16}O_2$ in the CI-Orbitrap compared to the CI-APi-TOF. This results in a more sensitive detection of the initially formed RO_2 radicals with relatively low oxygen content. It is important to mention that by applying the transmission curve to the CI-Orbitrap data, a larger discrepancy exist between the results of both instruments, see Figure S6. This discrepancy is obviously due to the different ion transmission corrections. Indeed, using the parameters selected in this study the ion transmission within the Orbitrap exhibit a steep increase between from *m/z* 60 to 300 Th (SI). However, much more experimental effort is needed in the future for a reliable determination of the ion transmission of both instruments and for different reagent ions. Hence it would be possible to determine i) how good the duty cycle correction accounts for the overall ion transmission of the CI-APi-TOF and ii) what is the accuracy of the depletion methods in comparison to absolute calibration methods.

Overall, the side-by-side comparison displays a very good agreement of the results of the CI-Orbitrap and the CI-APi-TOF with the exception of the lowest oxidized reaction products. By using the "sigmoidal correction function", 1.85×10^9 molecules cm^{-3}as the calibration factor for an AGC

target of 1 $\times 10^5$ charges, the LoQ of the CI-Orbitrap can be as low as 1 $\times$ 10^5 molecules cm^{-3} at a 10-minute integration time.

Determination of cluster binding energy. In common CI-APi-TOF approaches, the organic molecules of interest are observed as molecular clusters with the reagent ion (e.g., with CH_3COO^- or n-$C_3H_7NH_3^+$), see also eq. (1) and (2). In order to provide an accurate quantification of the compounds of interest it is essential to constrain the sensitivity of the reagent ion to OVOCs. To reach this goal, characterizing any limitations when detecting the compounds of interest, including the ion–molecule collision limit and the ion–molecule reaction time is critical. The proficiency of any neutral molecule to bind to the reagent ion is directly linked to the binding energy of the adduct.

Accordingly, a weakly bound adduct can undergo declustering, i.e., collision-induced dissociation (CID), during the flight trough the mass analyzer. Ultimately, the binding energy of the adduct and the energy of the collisions with gas molecules in the mass spectrometer will define the survival probability of the adduct ions. To constrain this parameter, procedures based on CID measurement coupled to quantum chemical methods have been proposed to investigate the behavior of adducts at different collision energies.[43,44] Nonetheless, carrying out such measurements is challenging for the hundreds of different molecular ions, typically observed with a CI-APi-TOF, especially when molecular structures remain unknown and/or are highly complex. Therefore, to quantitatively constrain the effective binding energies of a wide range of OVOCs and RO_2 radicals, we employed the capability of the Orbitrap analyzer to perform untargeted MS^2 analyses. Hence, all ions were injected into the HCD cell, where they collide at a defined collision energy with N_2 molecules. The NCE was ramped up from 1 to 7 eV. During the declustering scans, all potentials upstream the HCD cell remained identical and only the NCE within the HCD cell incremented, thereby avoiding any changes in the ion transmission of the mass spectrometer.

An example of the declustering analysis is presented in Figure 6A for a set of typical oxidation products, for which the remaining fraction of individual ions is plotted as a function of the CE (retrieve for each ion based on their *m/z*). Following the approach previously proposed for iodide-based clusters,[43–45] a sigmoidal fit was applied to the acquired data (Figure S7), in order to obtain the following parameters: i) the collision energy at which half of the signal is removed (CE_{50}), and ii) the

maximum amplitude of the sigmoidal function (S_0), corresponding to the relative signal intensity that would be measured in absence of declustering processes during the transmission through the mass spectrometer. In Table S1, the CE_{50} values of the OH-derived OVOCs and OH-derived RO_2 produced from the OH radical-initiated oxidation of α-pinene are reported. While direct comparison with quantum chemical calculations is not directly possible due to the absence of information on the studied OVOCs, earlier studies indicate that the values reported in Table S1 are within a fairly good agreement for binding energies determined for isoprene-derived oxidation products measured with CI-APiTOF using protonated n-propylamine or acetate.[41,42] For example, Berndt et al.[42] have estimated binding energies of the HPALD-(n-$C_3H_7NH_3^+$) cluster ($C_5H_8O_3$) cluster and HPALD-CH_3COO^- cluster of 28.5 and 31.9 kcal mol^{-1}, respectively, which is close to the values determined for OVOCs and RO_2 radicals containing 3 oxygen atoms (Table S1) within this present study.

Following the method proposed in former studies,[43,44] we found that the maximum possible transmission for each compound clustered with protonated n-propylamine (n-$C_3H_7NH_3^+$) is reached at a binding energy of ~ 35 kcal mol^{-1}. This indicates that for cluster ions having a greater binding energy, the stability of the adduct will be sufficient to transit through the different ion optics without significant declustering losses. These results are in line with the side-by-side comparison, where the largest discrepancy is observed for the lowest oxygenated species (e.g., O,O-$C_{10}H_{15}O_2$; HO-$C_{10}H_{16}O_2$), i.e., the compounds with the lowest binding energy (Table S1). By optimizing the different voltages, the declustering processes occurring within the APi-TOF and/or within the Orbitrap can be reduced. Finally, it is interesting to note that earlier work, performing CID experiments using iodide-based chemistry, determined a similar threshold, i.e., ~ 30 kcal mol^{-1}.[44]

CONCLUSIONS

In this work, we demonstrated the capability of the CI-Orbitrap in measuring RO_2 radicals as well as OVOCs at atmospherically relevant concentrations and compared them to simultaneous CI-APi-TOF measurements. We explored the current limitations of this new analytical technique and demonstrated that these can be partially overcome through a careful determination of a sigmoidal correction function. In addition, to unambiguously identify OVOCs formed in the gas phase, the analysis by

means of the CI-Orbitrap is able to accurately quantify organic species at concentration down to 1 × 10^5 molecules cm^{-3}. This LoQ is ~ one order of magnitude higher in comparison to the APi-TOF used in this study. In addition to the much greater mass resolving power, another clear advantage over the APi-TOF technique is the capability of performing MS^2 analyses needed to retrieve information on the chemical structure of the compounds of interest and to determine the binding energy of the clusters. Overall, the combination of high-mass resolving power of the Orbitrap and high sensitivity of the aminium/ammonium CI represents a powerful analytical tool that can improve our current knowledge regarding the complexity of the atmospheric gaseous composition. Thus, this new technique can help to answer some of the questions that so far were unable to be answered due to the pre-existing instrument limitations.

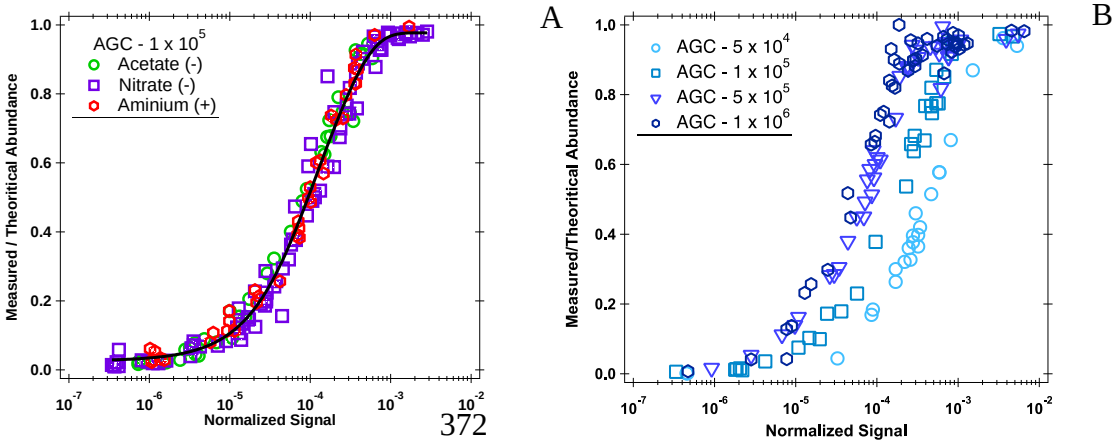

372

373 **Figure 1.** (**A**) Linearity of the Orbitrap as a function of normalized signal measured with protonated n-
374 propylamine (n-$C_3H_7NH_3^+$) and acetate (CH_3COO^-) reagent ions with the Orbitrap-Tropos and nitrate-
375 ion based chemistry with the Orbitrap-IRCELYON, using identical parameter settings. All signal
376 intensities were corrected with respect to the sum of $(CH_3COOH)_n$-CH_3COO^- (n = 0,1) at nominal 59
377 Th and 119 Th; to the sum of $(n\text{-}C_3H_7NH_2)_m$-n-$C_3H_7NH_3^+$ (m = 0,1) at nominal 60 Th and 119 Th; and
378 to the sum of $(HNO_3)_p$-NO_3^- (p = 0,1,2) at nominal 62, 125, 188 Th, for the respective reagent ions.
379 The black fit is the "sigmoidal correction function" based on a sigmoidal fitting algorithm. (**B**) Impact
380 of the AGC target on the linearity of the CI-Orbitrap-Tropos using aminium (n-$C_3H_7NH_3^+$) as the
381 reagent ion.
382

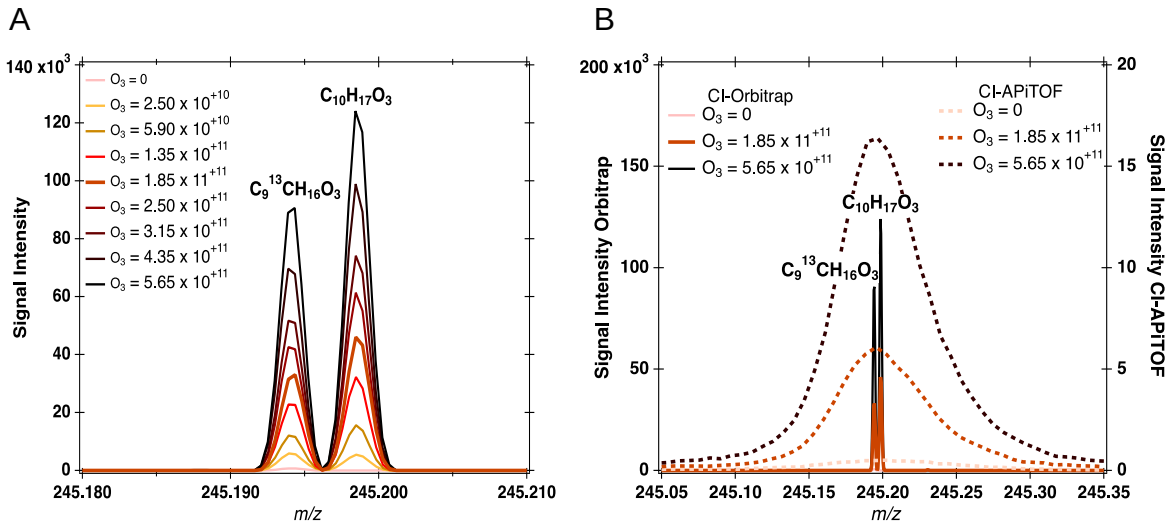

Figure 2. Mass spectra of ions at nominal *m/z* 245 from the combined ozonolysis and OH radical reaction of α-pinene for different reaction conditions (A) measured with the CI-Orbitrap and (B) comparison of the ion signals recorded by the CI-Orbitrap and the CI-APi-TOF. $C_9{}^{13}CH_{16}O_3$ represents most likely the ^{13}C-isotope of pinonaldehyde and $C_{10}H_{17}O_3$ the initial RO_2 radical from the OH attack, $HO\text{-}C_{10}H_{16}O_2$. Concentrations are given in molecules cm^{-3}.

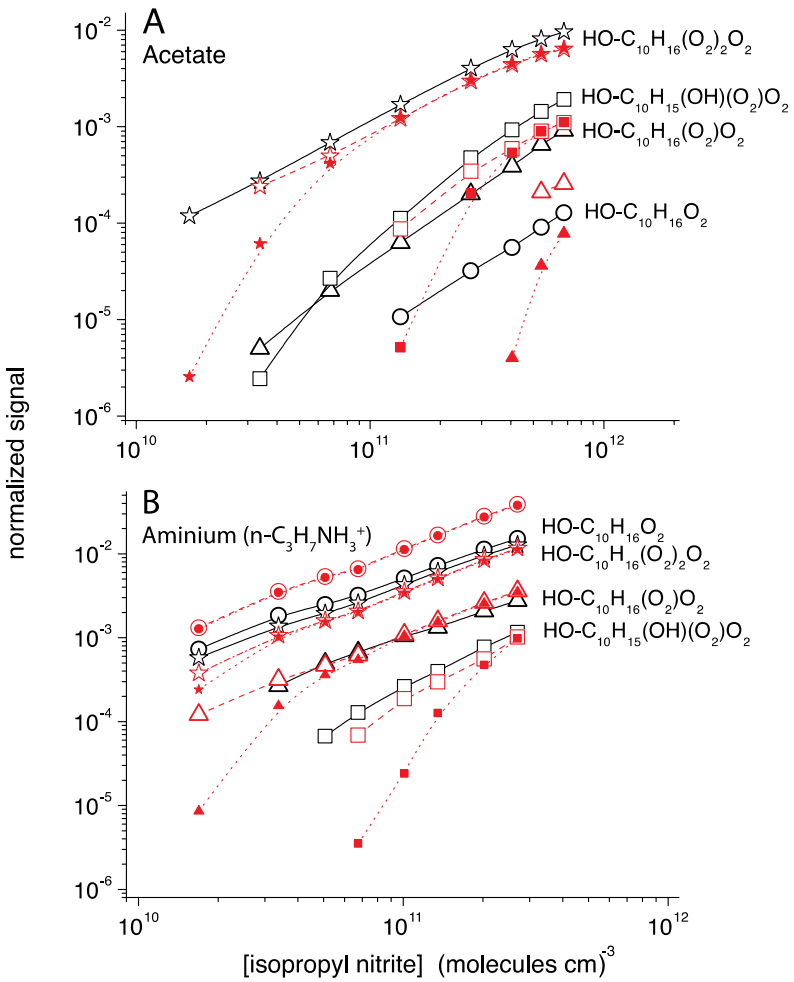

Figure 3. Normalized signals of RO_2 radicals produced from the OH radical-initiated oxidation of α-pinene as a function of initial IPN concentration measured by the CI-APi-TOF (black) and the CI-Orbitrap (red). OH radicals have been formed via IPN photolysis. Full and open markers in red correspond to raw and corrected (using the sigmoidal correction function) signals measured with the Orbitrap, respectively. (**A)** Acetate and (**B)** aminium ($n\text{-}C_3H_7NH_3^+$) served as the reagent ion for otherwise identical reaction conditions in both cases.

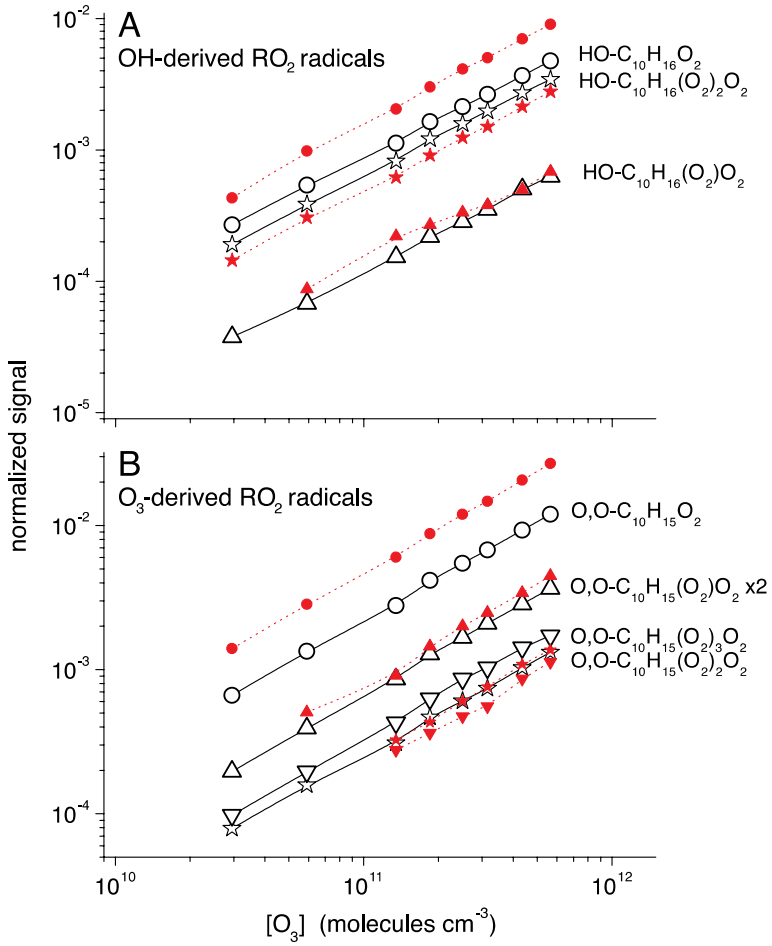

399

400 **Figure 4.** Normalized signals of **A)** OH-derived RO_2 radicals and **B)** O_3-derived RO_2 radicals
401 produced from the O_3/OH + α-pinene reaction as a function of the ozone concentration. Results
402 obtained by the CI-APi-TOF are given in black and those from the CI-Orbitrap in red using aminium
403 ($n\text{-}C_3H_7NH_3^+$) ionization in both cases. The Orbitrap data were corrected using the sigmoidal
404 correction function.

405

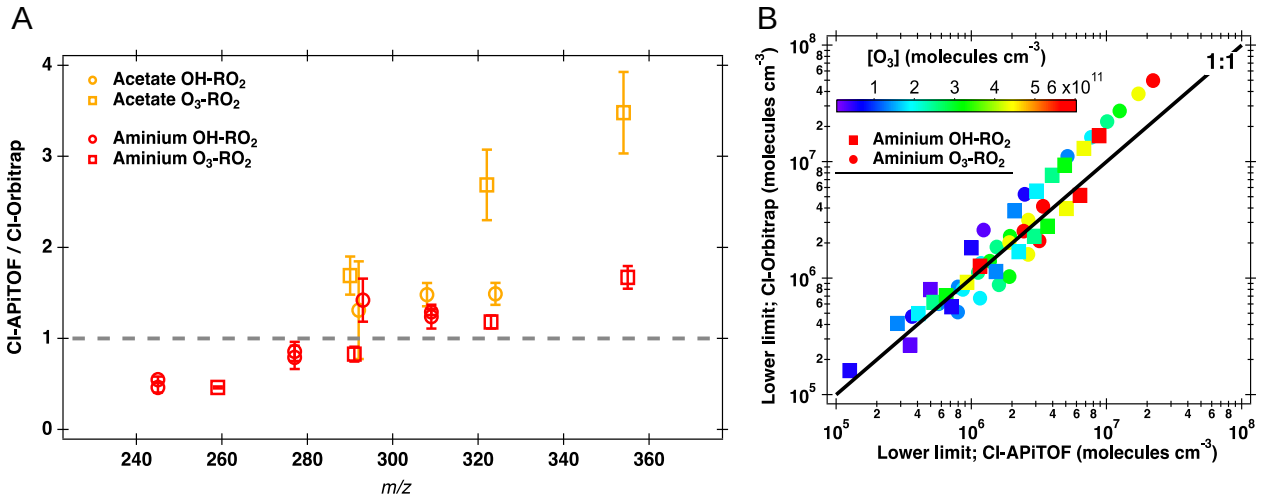

406

407 **Figure 5**. (A) Comparison between lower limit RO_2 radical concentrations measured with the CI-
408 APiTOF and the CI-Orbitrap in the different experiments. (B) Correlation of the concentrations of
409 RO_2 radicals formed from the O_3/OH + α-pinene reaction measured by the CI-APi-TOF and the CI-
410 Orbitrap using aminium ($n\text{-}C_3H_7NH_3^+$) ionization.

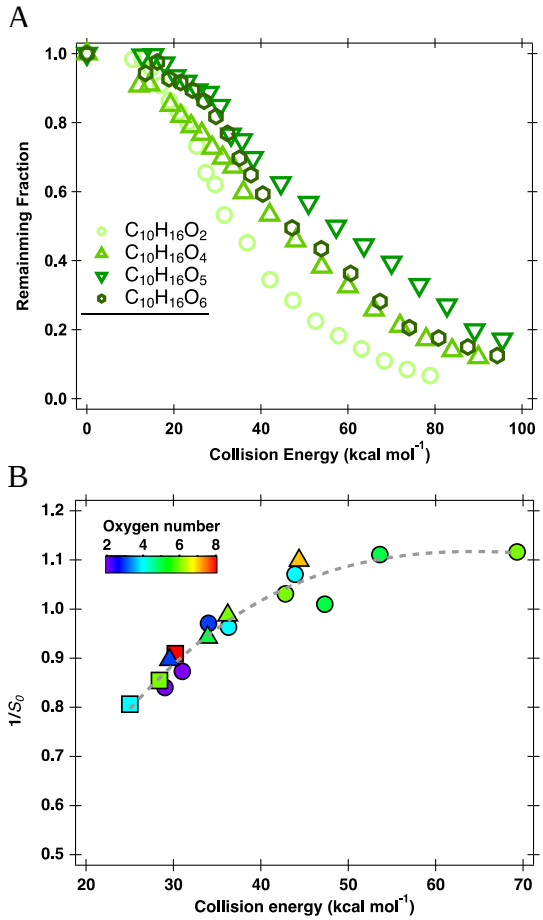

Figure 6. Declustering scans of (**A**) $C_{10}H_{16}O_{2\text{-}6}$ measured from the OH-initiated oxidation of α-pinene with the CI-Orbitrap using aminium (n-$C_3H_7NH_3^+$). (**B**) Relationship between fitting declustering scans ($1/S_0$) as a function of collision energy. CE_{50} is used as a measured of the relative binding energy and corresponds to the collision energy where half of the signal is removed. S_0 is the maximum amplitude obtained from the sigmoidal fit of declustering scans (e.g., Figure S7) of RO_2 radicals (triangle markers) and OVOCs (ON: square markers; non-ON: circle markers) formed from OH-initiated oxidation of α-pinene with the CI-Orbitrap using aminium (n-$C_3H_7NH_3^+$).

AUTHOR INFORMATION

Corresponding Authors

* E-mail (M. R.): matthieu.riva@ircelyon.univ-lyon1.fr

* E-mail (T. B.): berndt@tropos.de

ACKNOWLEDGMENTS

M.R. wishes to thank the French National program LEFE (Les Enveloppes Fluides et l'Environnement), for their financial support. This research project has received funding from the European Union's Horizon 2020 research and innovation program under grant agreement N^{o} 730997. The authors wish to thank Frederic Bourgain for technical support.

SUPPORTING INFORMATION

Figure S1 depicts the schematic of a Q Exactive mass spectrometer. Figure S2 shows the mass spectra of ions at *m/z* 245 and 260 measured during the oxidation of α-pinene. Figures S3 and S4 present the normalized signals of the organic nitrates and carbonyls produced from the OH-initiated oxidation of α-pinene, respectively. Figure S4 shows the correlation of the concentration measured species using both instruments and formed from the OH radical initiated oxidation of α-pinene using acetate-ion-based (CH_3COO^-) ionization. Figure S6 presents the normalized signals of RO_2 generated from the oxidation of α-pinene measured using aminium (n-$C_3H_7NH_3^+$). Figure S7 presents the declustering experiments performed on OVOCs formed from α-pinene ozonolysis. Figure S8 shows the mass Spectra of the different perfluorinated acids measured with CI-Orbitrap. Figure S9 presents the relative ion transmission fit determined using the depletion method. The Supporting Information is available free of charge on the ACS Publications website.

REFERENCES

(1) Hallquist, M.; Wenger, J. C.; Baltensperger, U.; Rudich, Y.; Simpson, D.; Claeys, M.; Dommen, J.; Donahue, N. M.; George, C.; Goldstein, A. H.; Hamilton, J. F.; Herrmann, H.; Hoffmann, T.; Iinuma, Y.; Jang, M.; Jenkin, M. E.; Jimenez, J. L.; Kiendler-Scharr, A.; Maenhaut, W.; McFiggans, G.; Mentel, Th. F.; Monod, A.; Prévôt, A. S. H.; Seinfeld, J. H.; Surratt, J. D.; Szmigielski, R.; Wildt, J. The Formation, Properties and Impact of Secondary Organic Aerosol: Current and Emerging Issues. *Atmospheric Chemistry and Physics* **2009**, *9* (14), 5155–5236. https://doi.org/10.5194/acp-9-5155-2009.

(2) Shrivastava, M.; Cappa, C. D.; Fan, J.; Goldstein, A. H.; Guenther, A. B.; Jimenez, J. L.; Kuang, C.; Laskin, A.; Martin, S. T.; Ng, N. L.; Petaja, T.; Pierce, J. R.; Rasch, P. J.; Roldin, P.; Seinfeld, J. H.; Shilling, J.; Smith, J. N.; Thornton, J. A.; Volkamer, R.; Wang, J.; Worsnop, D. R.; Zaveri, R. A.; Zelenyuk, A.; Zhang, Q. Recent Advances in Understanding Secondary Organic Aerosol: Implications for Global Climate Forcing: Advances in Secondary Organic Aerosol. *Reviews of Geophysics* **2017**, *55* (2), 509–559. https://doi.org/10.1002/2016RG000540.

(3) Wennberg, P. O.; Bates, K. H.; Crounse, J. D.; Dodson, L. G.; McVay, R. C.; Mertens, L. A.; Nguyen, T. B.; Praske, E.; Schwantes, R. H.; Smarte, M. D.; St Clair, J. M.; Teng, A. P.; Zhang, X.; Seinfeld, J. H. Gas-Phase Reactions of Isoprene and Its Major Oxidation Products. *Chemical Reviews*

2018. https://doi.org/10.1021/acs.chemrev.7b00439.

(4) Li, H.; Riva, M.; Rantala, P.; Heikkinen, L.; Daellenbach, K.; Krechmer, J. E.; Flaud, P.-M.; Worsnop, D.; Kulmala, M.; Villenave, E.; Perraudin, E.; Ehn, M.; Bianchi, F. Terpenes and Their Oxidation Products in the French Landes Forest: Insights from Vocus PTR-TOF Measurements. *Atmos. Chem. Phys.* **2020**, *20* (4), 1941–1959. https://doi.org/10.5194/acp-20-1941-2020.

(5) Jimenez, J. L.; Canagaratna, M. R.; Donahue, N. M.; Prevot, A. S. H.; Zhang, Q.; Kroll, J. H.; DeCarlo, P. F.; Allan, J. D.; Coe, H.; Ng, N. L.; Aiken, A. C.; Docherty, K. S.; Ulbrich, I. M.; Grieshop, A. P.; Robinson, A. L.; Duplissy, J.; Smith, J. D.; Wilson, K. R.; Lanz, V. A.; Hueglin, C.; Sun, Y. L.; Tian, J.; Laaksonen, A.; Raatikainen, T.; Rautiainen, J.; Vaattovaara, P.; Ehn, M.; Kulmala, M.; Tomlinson, J. M.; Collins, D. R.; Cubison, M. J.; E.; Dunlea, J.; Huffman, J. A.; Onasch, T. B.; Alfarra, M. R.; Williams, P. I.; Bower, K.; Kondo, Y.; Schneider, J.; Drewnick, F.; Borrmann, S.; Weimer, S.; Demerjian, K.; Salcedo, D.; Cottrell, L.; Griffin, R.; Takami, A.; Miyoshi, T.; Hatakeyama, S.; Shimono, A.; Sun, J. Y.; Zhang, Y. M.; Dzepina, K.; Kimmel, J. R.; Sueper, D.; Jayne, J. T.; Herndon, S. C.; Trimborn, A. M.; Williams, L. R.; Wood, E. C.; Middlebrook, A. M.; Kolb, C. E.; Baltensperger, U.; Worsnop, D. R. Evolution of Organic Aerosols in the Atmosphere. *Science* **2009**, *326* (5959), 1525–1529. https://doi.org/10.1126/science.1180353.

(6) Kirkby, J.; Duplissy, J.; Sengupta, K.; Frege, C.; Gordon, H.; Williamson, C.; Heinritzi, M.; Simon, M.; Yan, C.; Almeida, J.; Tröstl, J.; Nieminen, T.; Ortega, I. K.; Wagner, R.; Adamov, A.; Amorim, A.; Bernhammer, A.-K.; Bianchi, F.; Breitenlechner, M.; Brilke, S.; Chen, X.; Craven, J.; Dias, A.; Ehrhart, S.; Flagan, R. C.; Franchin, A.; Fuchs, C.; Guida, R.; Hakala, J.; Hoyle, C. R.; Jokinen, T.; Junninen, H.; Kangasluoma, J.; Kim, J.; Krapf, M.; Kürten, A.; Laaksonen, A.; Lehtipalo, K.; Makhmutov, V.; Mathot, S.; Molteni, U.; Onnela, A.; Peräkylä, O.; Piel, F.; Petäjä, T.; Praplan, A. P.; Pringle, K.; Rap, A.; Richards, N. A. D.; Riipinen, I.; Rissanen, M. P.; Rondo, L.; Sarnela, N.; Schobesberger, S.; Scott, C. E.; Seinfeld, J. H.; Sipilä, M.; Steiner, G.; Stozhkov, Y.; Stratmann, F.; Tomé, A.; Virtanen, A.; Vogel, A. L.; Wagner, A. C.; Wagner, P. E.; Weingartner, E.; Wimmer, D.; Winkler, P. M.; Ye, P.; Zhang, X.; Hansel, A.; Dommen, J.; Donahue, N. M.; Worsnop, D. R.; Baltensperger, U.; Kulmala, M.; Carslaw, K. S.; Curtius, J. Ion-Induced Nucleation of Pure Biogenic Particles. *Nature* **2016**, *533* (7604), 521–526. https://doi.org/10.1038/nature17953.

(7) Ehn, M.; Thornton, J. A.; Kleist, E.; Sipilä, M.; Junninen, H.; Pullinen, I.; Springer, M.; Rubach, F.; Tillmann, R.; Lee, B.; Lopez-Hilfiker, F.; Andres, S.; Acir, I.-H.; Rissanen, M.; Jokinen, T.; Schobesberger, S.; Kangasluoma, J.; Kontkanen, J.; Nieminen, T.; Kurtén, T.; Nielsen, L. B.; Jørgensen, S.; Kjaergaard, H. G.; Canagaratna, M.; Maso, M. D.; Berndt, T.; Petäjä, T.; Wahner, A.; Kerminen, V.-M.; Kulmala, M.; Worsnop, D. R.; Wildt, J.; Mentel, T. F. A Large Source of Low-Volatility Secondary Organic Aerosol. *Nature* **2014**, *506* (7489), 476–479. https://doi.org/10.1038/nature13032.

(8) Bianchi, F.; Kurtén, T.; Riva, M.; Mohr, C.; Rissanen, M. P.; Roldin, P.; Berndt, T.; Crounse, J. D.; Wennberg, P. O.; Mentel, T. F.; Wildt, J.; Junninen, H.; Jokinen, T.; Kulmala, M.; Worsnop, D. R.; Thornton, J. A.; Donahue, N.; Kjaergaard, H. G.; Ehn, M. Highly Oxygenated Organic Molecules (HOM) from Gas-Phase Autoxidation Involving Peroxy Radicals: A Key Contributor to Atmospheric Aerosol. *Chemical Reviews* **2019**. https://doi.org/10.1021/acs.chemrev.8b00395.

(9) Crounse, J. D.; Nielsen, L. B.; Jørgensen, S.; Kjaergaard, H. G.; Wennberg, P. O. Autoxidation of Organic Compounds in the Atmosphere. *The Journal of Physical Chemistry Letters* **2013**, *4* (20), 3513–3520. https://doi.org/10.1021/jz4019207.

(10) Berndt, T.; Scholz, W.; Mentler, B.; Fischer, L.; Herrmann, H.; Kulmala, M.; Hansel, A. Accretion Product Formation from Self- and Cross-Reactions of RO_2 Radicals in the Atmosphere. *Angewandte Chemie International Edition* **2018**, *57* (14), 3820–3824. https://doi.org/10.1002/anie.201710989.

(11) Berndt, T.; Richters, S.; Kaethner, R.; Voigtländer, J.; Stratmann, F.; Sipilä, M.; Kulmala, M.; Herrmann, H. Gas-Phase Ozonolysis of Cycloalkenes: Formation of Highly Oxidized RO_2 Radicals and Their Reactions with NO, NO_2, SO_2, and Other RO_2 Radicals. *The Journal of Physical Chemistry A* **2015**, *119* (41), 10336–10348. https://doi.org/10.1021/acs.jpca.5b07295.

(12) Rissanen, M. P.; Kurtén, T.; Sipilä, M.; Thornton, J. A.; Kangasluoma, J.; Sarnela, N.; Junninen, H.; Jørgensen, S.; Schallhart, S.; Kajos, M. K.; Taipale, R.; Springer, M.; Mentel, T. F.; Ruuskanen, T.; Petäjä, T.; Worsnop, D. R.; Kjaergaard, H. G.; Ehn, M. The Formation of Highly Oxidized Multifunctional Products in the Ozonolysis of Cyclohexene. *Journal of the American Chemical Society* **2014**, *136* (44), 15596–15606. https://doi.org/10.1021/ja507146s.

(13) Jokinen, T.; Sipilä, M.; Richters, S.; Kerminen, V.-M.; Paasonen, P.; Stratmann, F.; Worsnop, D.; Kulmala, M.; Ehn, M.; Herrmann, H.; Berndt, T. Rapid Autoxidation Forms Highly Oxidized RO_2 Radicals in the Atmosphere. *Angewandte Chemie International Edition* **2014**, *53* (52), 14596–14600. https://doi.org/10.1002/anie.201408566.

(14) Jokinen, T.; Berndt, T.; Makkonen, R.; Kerminen, V.-M.; Junninen, H.; Paasonen, P.; Stratmann, F.; Herrmann, H.; Guenther, A. B.; Worsnop, D. R.; Kulmala, M.; Ehn, M.; Sipilä, M. Production of Extremely Low Volatile Organic Compounds from Biogenic Emissions: Measured Yields and Atmospheric Implications. *Proceedings of the National Academy of Sciences* **2015**, *112* (23), 7123–7128. https://doi.org/10.1073/pnas.1423977112.

(15) Wang, S.; Riva, M.; Yan, C.; Ehn, M.; Wang, L. Primary Formation of Highly Oxidized Multifunctional Products in the OH-Initiated Oxidation of Isoprene. A Combined Theoretical and Experimental Study. *Environmental Science & Technology* **2018**. https://doi.org/10.1021/acs.est.8b02783.

(16) Ziemann, P. J.; Atkinson, R. Kinetics, Products, and Mechanisms of Secondary Organic Aerosol Formation. *Chemical Society Reviews* **2012**, *41* (19), 6582. https://doi.org/10.1039/c2cs35122f.

(17) McFiggans, G.; Mentel, T. F.; Wildt, J.; Pullinen, I.; Kang, S.; Kleist, E.; Schmitt, S.; Springer, M.; Tillmann, R.; Wu, C.; Zhao, D.; Hallquist, M.; Faxon, C.; Le Breton, M.; Hallquist, Å. M.; Simpson, D.; Bergström, R.; Jenkin, M. E.; Ehn, M.; Thornton, J. A.; Alfarra, M. R.; Bannan, T. J.; Percival, C. J.; Priestley, M.; Topping, D.; Kiendler-Scharr, A. Secondary Organic Aerosol Reduced by Mixture of Atmospheric Vapours. *Nature* **2019**, *565* (7741), 587–593. https://doi.org/10.1038/s41586-018-0871-y.

(18) Riva, M.; Rantala, P.; Krechmer, J. E.; Peräkylä, O.; Zhang, Y.; Heikkinen, L.; Garmash, O.; Yan, C.; Kulmala, M.; Worsnop, D.; Ehn, M. Evaluating the Performance of Five Different Chemical Ionization Techniques for Detecting Gaseous Oxygenated Organic Species. *Atmospheric Measurement Techniques Discussions* **2018**, 1–39. https://doi.org/10.5194/amt-2018-407.

(19) Krechmer, J.; Lopez-Hilfiker, F.; Koss, A.; Hutterli, M.; Stoermer, C.; Deming, B.; Kimmel, J.; Warneke, C.; Holzinger, R.; Jayne, J. T.; Worsnop, D. R.; Fuhrer, K.; Gonin, M.; de Gouw, J. A. Evaluation of a New Reagent-Ion Source and Focusing Ion-Molecule Reactor for Use in Proton-Transfer-Reaction Mass Spectrometry. *Analytical Chemistry* **2018**. https://doi.org/10.1021/acs.analchem.8b02641.

(20) Breitenlechner, M.; Fischer, L.; Hainer, M.; Heinritzi, M.; Curtius, J.; Hansel, A. PTR3: An Instrument for Studying the Lifecycle of Reactive Organic Carbon in the Atmosphere. *Analytical Chemistry* **2017**, *89* (11), 5824–5831. https://doi.org/10.1021/acs.analchem.6b05110.

(21) Jokinen, T.; Sipilä, M.; Junninen, H.; Ehn, M.; Lönn, G.; Hakala, J.; Petäjä, T.; Mauldin, R. L.; Kulmala, M.; Worsnop, D. R. Atmospheric Sulphuric Acid and Neutral Cluster Measurements

Using CI-APi-TOF. *Atmospheric Chemistry and Physics* **2012**, *12* (9), 4117–4125. https://doi.org/10.5194/acp-12-4117-2012.

(22) Lee, B. H.; Lopez-Hilfiker, F. D.; Mohr, C.; Kurtén, T.; Worsnop, D. R.; Thornton, J. A. An Iodide-Adduct High-Resolution Time-of-Flight Chemical-Ionization Mass Spectrometer: Application to Atmospheric Inorganic and Organic Compounds. *Environmental Science & Technology* **2014**, *48* (11), 6309–6317. https://doi.org/10.1021/es500362a.

(23) Crounse, J. D.; McKinney, K. A.; Kwan, A. J.; Wennberg, P. O. Measurement of Gas-Phase Hydroperoxides by Chemical Ionization Mass Spectrometry. *Analytical Chemistry* **2006**, *78* (19), 6726–6732. https://doi.org/10.1021/ac0604235.

(24) Berndt, T.; Richters, S.; Jokinen, T.; Hyttinen, N.; Kurtén, T.; Otkjær, R. V.; Kjaergaard, H. G.; Stratmann, F.; Herrmann, H.; Sipilä, M.; Kulmala, M.; Ehn, M. Hydroxyl Radical-Induced Formation of Highly Oxidized Organic Compounds. *Nat Commun* **2016**, *7* (1), 13677. https://doi.org/10.1038/ncomms13677.

(25) Berndt, T.; Herrmann, H.; Kurtén, T. Direct Probing of Criegee Intermediates from Gas-Phase Ozonolysis Using Chemical Ionization Mass Spectrometry. *Journal of the American Chemical Society* **2017**, *139* (38), 13387–13392. https://doi.org/10.1021/jacs.7b05849.

(26) Hansel, A.; Scholz, W.; Mentler, B.; Fischer, L.; Berndt, T. Detection of RO 2 Radicals and Other Products from Cyclohexene Ozonolysis with NH 4 + and Acetate Chemical Ionization Mass Spectrometry. *Atmospheric Environment* **2018**, *186*, 248–255. https://doi.org/10.1016/j.atmosenv.2018.04.023.

(27) Cubison, M. J.; Jimenez, J. L. Statistical Precision of the Intensities Retrieved from Constrained Fitting of Overlapping Peaks in High-Resolution Mass Spectra. *Atmospheric Measurement Techniques* **2015**, *8* (6), 2333–2345. https://doi.org/10.5194/amt-8-2333-2015.

(28) Stark, H.; Yatavelli, R. L. N.; Thompson, S. L.; Kimmel, J. R.; Cubison, M. J.; Chhabra, P. S.; Canagaratna, M. R.; Jayne, J. T.; Worsnop, D. R.; Jimenez, J. L. Methods to Extract Molecular and Bulk Chemical Information from Series of Complex Mass Spectra with Limited Mass Resolution. *International Journal of Mass Spectrometry* **2015**, *389*, 26–38. https://doi.org/10.1016/j.ijms.2015.08.011.

(29) Zhang, Y.; Peräkylä, O.; Yan, C.; Heikkinen, L.; Äijälä, M.; Daellenbach, K. R.; Zha, Q.; Riva, M.; Garmash, O.; Junninen, H.; Paatero, P.; Worsnop, D.; Ehn, M. A Novel Approach for Simple Statistical Analysis of High-Resolution Mass Spectra. *Atmos. Meas. Tech.* **2019**, *12* (7), 3761–3776. https://doi.org/10.5194/amt-12-3761-2019.

(30) Riva, M.; Ehn, M.; Li, D.; Tomaz, S.; Bourgain, F.; Perrier, S.; George, C. CI-Orbitrap: An Analytical Instrument To Study Atmospheric Reactive Organic Species. *Anal. Chem.* **2019**, *91* (15), 9419–9423. https://doi.org/10.1021/acs.analchem.9b02093.

(31) Eisele, F. L.; Tanner, D. J. Measurement of the Gas Phase Concentration of H_2SO_4 and Methane Sulfonic Acid and Estimates of H_2SO_4 Production and Loss in the Atmosphere. *Journal of Geophysical Research: Atmospheres* **1993**, *98* (D5), 9001–9010. https://doi.org/10.1029/93JD00031.

(32) Michalski, A.; Damoc, E.; Hauschild, J.-P.; Lange, O.; Wieghaus, A.; Makarov, A.; Nagaraj, N.; Cox, J.; Mann, M.; Horning, S. Mass Spectrometry-Based Proteomics Using Q Exactive, a High-Performance Benchtop Quadrupole Orbitrap Mass Spectrometer. *Molecular & Cellular Proteomics* **2011**, *10* (9), M111.011015. https://doi.org/10.1074/mcp.M111.011015.

(33) Zuth, C.; Vogel, A. L.; Ockenfeld, S.; Huesmann, R.; Hoffmann, T. Ultrahigh-Resolution

Mass Spectrometry in Real Time: Atmospheric Pressure Chemical Ionization Orbitrap Mass Spectrometry of Atmospheric Organic Aerosol. *Analytical Chemistry* **2018**, *90* (15), 8816–8823. https://doi.org/10.1021/acs.analchem.8b00671.

(34) Berresheim, H.; Elste, T.; Plass-Dülmer, C.; Eiseleb, F. L.; Tannerb, D. J. Chemical Ionization Mass Spectrometer for Long-Term Measurements of Atmospheric OH and H2SO4. *International Journal of Mass Spectrometry* **2000**, *202* (1–3), 91–109. https://doi.org/10.1016/S1387-3806(00)00233-5.

(35) Berndt, T.; Mentler, B.; Scholz, W.; Fischer, L.; Herrmann, H.; Kulmala, M.; Hansel, A. Accretion Product Formation from Ozonolysis and OH Radical Reaction of α-Pinene: Mechanistic Insight and the Influence of Isoprene and Ethylene. *Environ. Sci. Technol.* **2018**, *52* (19), 11069–11077. https://doi.org/10.1021/acs.est.8b02210.

(36) Heinritzi, M.; Simon, M.; Steiner, G.; Wagner, A. C.; Kürten, A.; Hansel, A.; Curtius, J. Characterization of the Mass-Dependent Transmission Efficiency of a CIMS. *Atmospheric Measurement Techniques* **2016**, *9* (4), 1449–1460. https://doi.org/10.5194/amt-9-1449-2016.

(37) Junninen, H.; Ehn, M.; Petäjä, T.; Luosujärvi, L.; Kotiaho, T.; Kostiainen, R.; Rohner, U.; Gonin, M.; Fuhrer, K.; Kulmala, M.; Worsnop, D. R. A High-Resolution Mass Spectrometer to Measure Atmospheric Ion Composition. *Atmospheric Measurement Techniques* **2010**, *3* (4), 1039–1053. https://doi.org/10.5194/amt-3-1039-2010.

(38) Ehn, M.; Junninen, H.; Schobesberger, S.; Manninen, H. E.; Franchin, A.; Sipilä, M.; Petäjä, T.; Kerminen, V.-M.; Tammet, H.; Mirme, A.; Mirme, S.; Hõrrak, U.; Kulmala, M.; Worsnop, D. R. An Instrumental Comparison of Mobility and Mass Measurements of Atmospheric Small Ions. *Aerosol Science and Technology* **2011**, *45* (4), 522–532. https://doi.org/10.1080/02786826.2010.547890.

(39) Eiler, J.; Cesar, J.; Chimiak, L.; Dallas, B.; Grice, K.; Griep-Raming, J.; Juchelka, D.; Kitchen, N.; Lloyd, M.; Makarov, A.; Robins, R.; Schwieters, J. Analysis of Molecular Isotopic Structures at High Precision and Accuracy by Orbitrap Mass Spectrometry. *International Journal of Mass Spectrometry* **2017**, *422*, 126–142. https://doi.org/10.1016/j.ijms.2017.10.002.

(40) Makarov, A.; Denisov, E. Dynamics of Ions of Intact Proteins in the Orbitrap Mass Analyzer. *J Am Soc Mass Spectrom* **2009**, *20* (8), 1486–1495. https://doi.org/10.1016/j.jasms.2009.03.024.

(41) Hyttinen, N.; Otkjær, R. V.; Iyer, S.; Kjaergaard, H. G.; Rissanen, M. P.; Wennberg, P. O.; Kurtén, T. Computational Comparison of Different Reagent Ions in the Chemical Ionization of Oxidized Multifunctional Compounds. *The Journal of Physical Chemistry A* **2018**, *122* (1), 269–279. https://doi.org/10.1021/acs.jpca.7b10015.

(42) Berndt, T.; Hyttinen, N.; Herrmann, H.; Hansel, A. First Oxidation Products from the Reaction of Hydroxyl Radicals with Isoprene for Pristine Environmental Conditions. *Commun Chem* **2019**, *2* (1), 21. https://doi.org/10.1038/s42004-019-0120-9.

(43) Isaacman-VanWertz, G.; Massoli, P.; O'Brien, R.; Lim, C.; Franklin, J. P.; Moss, J. A.; Hunter, J. F.; Nowak, J. B.; Canagaratna, M. R.; Misztal, P. K.; Arata, C.; Roscioli, J. R.; Herndon, S. T.; Onasch, T. B.; Lambe, A. T.; Jayne, J. T.; Su, L.; Knopf, D. A.; Goldstein, A. H.; Worsnop, D. R.; Kroll, J. H. Chemical Evolution of Atmospheric Organic Carbon over Multiple Generations of Oxidation. *Nature Chemistry* **2018**, *10* (4), 462–468. https://doi.org/10.1038/s41557-018-0002-2.

(44) Lopez-Hilfiker, F. D.; Iyer, S.; Mohr, C.; Lee, B. H.; D'Ambro, E. L.; Kurtén, T.; Thornton, J. A. Constraining the Sensitivity of Iodide Adduct Chemical Ionization Mass Spectrometry to Multifunctional Organic Molecules Using the Collision Limit and Thermodynamic Stability of Iodide Ion Adducts. *Atmospheric Measurement Techniques* **2016**, *9* (4), 1505–1512.

https://doi.org/10.5194/amt-9-1505-2016.

(45) Iyer, S.; Lopez-Hilfiker, F.; Lee, B. H.; Thornton, J. A.; Kurtén, T. Modeling the Detection of Organic and Inorganic Compounds Using Iodide-Based Chemical Ionization. *The Journal of Physical Chemistry A* **2016**, *120* (4), 576–587. https://doi.org/10.1021/acs.jpca.5b09837.